Cyclin B Export to the Cytoplasm via the Nup62 Subcomplex and Its Subsequent Rapid Nuclear Import Are Required for the Initiation of Drosophila Male Meiosis

Kanta Yamazoe and Yoshihiro H. Inoue *

Posted Date: 12 October 2023

doi: 10.20944/preprints202310.0751.v1

Keywords: Drosophila; male meiosis; cyclin B; Cyclin-dependent kinase 1; Cyclin-dependent kinase inhibitors

Article

Cyclin B Export to the Cytoplasm via the Nup62 Subcomplex and Its Subsequent Rapid Nuclear Import Are Required for the Initiation of *Drosophila* Male Meiosis

Kanta Yamazoe and Yoshihiro H. Inoue *

Biomedical Research Center, Graduate School of Science and Technology, Kyoto Institute of Technology, Matsugasaki, Sakyo, Kyoto, 606-0962, Japan

* Correspondence: yhinoue@kit.ac.jp; Tel.: +8175-7247876

Abstract: The cyclin-dependent kinase (Cdk) 1–cyclin B (CycB) complex plays critical roles in cell cycle regulation. Before *Drosophila* male meiosis, CycB is exported from the nucleus to the cytoplasm via the nuclear porin 62kD (Nup62) subcomplex in the nuclear pore complex. When this is inhibited, Cdk1 is not activated, and meiosis does not initiate. We investigated the mechanism that controls cellular localization and activation of Cdk1. Cdk1–CycB continuously shuttled into and out of the nucleus in the prolonged G2 phase before meiosis. Overexpression of CycB, but not that with nuclear localization signal sequences, rescued reduced cytoplasmic CycB and inhibition of meiosis in *Nup62*-silenced cells. Full-scale Cdk1 activation occurred in the nucleus shortly after its rapid nuclear entry. Cdk1-dependent centrosome separation did not occur in *Nup62*-silenced cells, while Cdk1 interacted with Cdk-activating kinase and Twine/Cdc25C in the nucleus of *Nup62*-silenced cells, suggesting the involvement of another suppression mechanism. Silencing of *roughex* rescued Cdk1 inhibition and initiated meiosis. Nuclear exports of Cdk1 ensured its escape from inhibition by cyclin-dependent kinase inhibitor. The complex reentered the nucleus via importin β at the onset of meiosis. We propose a model regarding the dynamics and activation mechanism of Cdk1–CycB to initiate male meiosis.

Keywords: *Drosophila*; male meiosis; cyclin B; Cyclin-dependent kinase 1; Cyclin-dependent kinase inhibitors

1. Introduction

A conserved molecular mechanism that controls the initiation of cell division in eukaryotes involves the activation of a cyclin-dependent kinase 1 (Cdk1) that serves as a master regulator of the M-phase in mitosis and meiosis (Morgan, 2007, Albert, eds., 2017). In eukaryotes, the following three conditions are indispensable for activating protein kinase: complex formation with its regulatory subunit, Cyclin B (CycB), phosphorylation of Thr^{161} of Cdk1, and removal of phosphate groups from Thr^{14} and Tyr^{15}, both of which are involved in negative regulation of kinases phosphorylated by Wee1/ Myt1 (Liu, *et al*., 1997, Coulonval, *et al*., 2011, Ayeni, et al., 2014). Cdk1 is activated at the onset of M-phase by dephosphorylation of Thr^{14} and Tyr^{15} by Cell division cycle (Cdc) 25 orthologues. Thr^{161} of Cdk1 also needs to be phosphorylated by Cdk-activating kinase (CAK) (Kaldis, 1999). In addition to Cdk1 modification, another type of inhibitor known as Cdk inhibitors (CKIs), such as p21, plays an important role in controlling cell cycle. CKIs were originally identified as negative factors, which bind to suppress Cdk activity at the G1/S phase and also effective to CycB/Cdk1 during G2/M transition (Dulić, et al., 1998; Dash and El-Deiry, 2005). These inhibitors need to be released from Cdk1 before the onset of M-phase (Russo *et al*., 1996, Lim and Kaldis 2013). From later stages of the G2 phase towards the beginning of M-phase, Cdk1 activity depends on an increasing expression of CycB. *In vitro* assays using animal oocyte extracts have revealed that Cdks are activated progressively

 doi:10.20944/preprints202310.0751.v1

(Lindqvist *et al*., 2009; Qian *et al*., 2013; Hegarat *et al*., 2016). A small population of CycB–Cdk1 is first activated by a trigger (Hiraoka *et al*., 2019). Consequently, a balance between Cdc25 and Wee1/Myt1 activities is shifted so that Cdc25 activity becomes predominant. CycB–Cdk1 further accelerates its dephosphorylation via positive feedback loops, leading to maximal activation (Santos *et al*., 2012; Hegarat *et al*., 2016; Maryu and Yang, 2022). By contrast, a double-negative feedback loop implemented by inactivation of counteracting phosphatase by Cdk1 also contributes to its own activation (Crncec and Hochegger 2019). In addition, subcellular localization of Cdk1 and its regulatory factors, and their timing of migration to other compartments have been considered to be critical points for mitotic entry in mammalian cells (Pines and Hunter 1994, Hagting *et al* 1998, Porter and Donoghue 2003, Gavet and Pines 2010). In the G2 phase, CycB is enriched in the cytoplasm but continuously shuttles into and out of the nucleus until shortly before onset of mitosis (Gavet and Pines 2010). Mitosis is triggered by the activation of Cdk1–CycB and its translocation from the cytoplasm to the nucleus. The spatial and feedback regulation ensures a rapid and irreversible transition from interphase to mitosis.

Much progress has already been made in elucidating special regulation to control Cdk1 activation during G2/M transition in mitosis. By contrast, several issues should be uncovered regarding the mechanism of meiotic initiation. Meiosis is expected to be highly susceptible to spatial and temporal control of cell cycle in cooperation with developmental program. In mouse oocytes, for example, spatial regulation of Anaphase Promoting Complex (APC)/C^{Cdh1}-induced CycB degradation maintains G2 arrest of oocytes for several years (Holt *et al*., 2010). The stepwise activation of Cdk1 may rather play a more important role in meiosis than that in mitotic cell cycle. As the meiotic cycle in *Drosophila* is generally constituted of a prolonged G2-like growth period, the timing to initiate meiosis is expected to be strictly regulated. The mechanism of how the timing of Cdk1-dependent phosphorylation is determined shortly before the nuclear envelop breaks down still remains to be explored. With reference to the regulatory mechanisms of mitotic initiation, we can expect a similar regulation that initiates male meiosis in *Drosophila* (Sigrist, *et al*., 1995). In contrast, several specific regulations different from the core regulatory system take place during meiosis. For example, a Cdc25 orthologue encoded by *twine* plays a meiosis-specific role in activating Cdk1 before the onset of meiosis during oogenesis and spermatogenesis, while *string* is required at the initiation of mitotic events during embryogenesis and those of germline stem cells and their progenitor cells. (Courtot *et al*., 1992, Alphey, *et al*., 1992, White-Cooper, *et al*., 1993). *cycB* mRNA is expressed at low levels in the spermatogonia undergoing mitotic proliferation, downregulated after completion of mitotic divisions, and then re-expressed in high levels in spermatocytes during the growth phase before meiosis (White-Cooper *et al*., 1998). By contrast, their protein levels in spermatocytes remain low until spermatocytes enter the G2/M transition after the appearance of mRNA. *CycB* translation is repressed until before the onset of male meiosis (Baker *et al*., 2015) by two proteins that bind to *cycB* mRNA in spermatocytes. CycB accumulates in the cytoplasm prior to initiation of chromatin condensation, remains in high level during prometaphase, and then enters the nucleus at the onset of meiosis.

Drosophila spermatocytes before or undergoing meiosis I have several advantages with respect to the investigation of cell cycle regulation at the G2/M phase. Dissecting the gonads and identifying and observing meiotic cells are easy as the large cell size owing to remarkable cell growth facilitates the observation of subcellular localization of specific regulatory proteins (Inoue *et al*., 2012). Nevertheless, comparing among the spermatocytes in different cysts at a similar development stage was not easy. The growth phase has been classified into six stages, S1–6, based on the chromatin morphology and intracellular structure of premeiotic spermatocytes (Cenci *et al*., 1994). Recently, the characteristic size and morphology of the nucleolus in the growth phase have allowed us to precisely identify the developmental stages of spermatocytes (Azuma *et al*., 2021).

No spermatocytes undergoing meiosis have been observed in the testes harboring testis-specific depletion of components of Nup62 subcomplex composing the central channel of nuclear pore complex (NPC), while meiosis initiates normally in the testes harboring depletion of other NPC-subcomplexes (Hayashi *et al*., 2016). Silencing of *Nup62* using RNA interference results in the accumulation of CycB in the nucleus during the growth phase corresponding to a prolonged G2

 doi:10.20944/preprints202310.0751.v1

phase before initiation of meiosis, and thereby inhibits Cdk1 activation, leading to cell cycle arrest before male meiosis (Okazaki, et al., 2020). These results are inconsistent with previous results in that the precocious accumulation of CycB in the nucleus by expression of export-defective CycB does not influence mitotic entry (Hagting et al., 1998). This unexpected result highlights the importance of subcellular localization of CycB in cell cycle progression before male meiosis, and that selective nuclear-cytoplasmic transport of cell cycle regulators may be critical for determining the time of meiotic initiation (Okazaki et al., 2020). A constitutively active Cdk1 mutant ($Cdk1^{T14A\ Y15F}$) has failed to rescue the meiotic phenotype by *Nup62*-silencing, suggesting that the modification that removes inhibitory phosphorylation of Cdk1 does not take place in the absence of male meiosis (Okazaki et al. 2020). However, the mechanism of hampering of meiotic initiation owing to the inhibition of nuclear export of CycB remains unclear.

In this study, we aimed to address several issues regarding the initiation of male meiosis in *Drosophila*. We performed a time-lapse observation of living premeiotic spermatocytes to investigate whether CycB continuously shuttles between the nucleus and cytoplasm before meiosis. Furthermore, we investigated the subcellular localization of positive regulators and their possible complexes with Cdk1. We also examined whether negative regulators were involved in inhibiting nuclear export of Cdk1 and its activation by RNA interference. Additionally, we examined whether importin β is required for reentry of Cdk1 into the nucleus.

2. Materials and Methods

2.1. Drosophila stocks

We used the following *UAS-RNAi* stocks for RNAi experiments; *P{KK108318}VIE-260B* (VDRC#100588) were used for a depletion of *Nup62* (Okazaki et al., 2020), *P{TRiP.GL00262} (BDSC#35350)* for a depletion of *Cdk1 (Huang et al., 2021), P{TRiP.HMS00467} (BDSC# 32467)* for a depletion of *rux (*Ni, *et al.,* 2011*). P{TRiP.GL01273} (BDSC#41845)* was used a depletion of *Fs(2)Ketel (*Khalil, *et al.,* 2022*).* These RNAi stocks were obtained from Bloomington Drosophila stock center (Indiana University, Bloomington, USA). To visualize Cyclin B (CycB) in living spermatocytes, *P{Ubi-p63E-CycB.GFP}* was used (Huang and Raff., 1999, a gift from J. Raff (University of Oxford, Oxford, UK)). We used *M{UAS-CycB.ORF.3xHA}* (#F001154, Fly-ORF (University of Zurich, Zurich, Switzerland)) for overexpression of normal CycB (Schertel *et al*., 2013). We also used *P{twe-EGFP}* (Liu *et al*., 2020, a gift from J. Großhans (The Philipps University of Marburg, Marburg, Germany)) to express GFP-tagged Twine. To overexpress Wee1 and Myt1, we used *P{UASp-Wee1.VFP}2* (BDSC#65390) and *P{UASp-EGFP-Myt1}1* (BDSC#65393). For induction of various dsRNA against endogenous mRNA in spermatocytes, we used *P{UAS-dcr2}; P{bam-GAL4::VP16}* (*bam-Gal4*) (Hayashi *et al*., 2016). As a control, F1 progenies from a genetic cross between *bam-Gal4* and *w* were used and noted as *bam*>+. *P{Sa-GFP}* was used as a maker to determine the stage of the growth phase of spermatocytes (Azuma *et al*., 2021). All *Drosophila melanogaster* stocks were maintained on standard cornmeal food at 25°C as previously described (Oka *et al*., 2015). For efficient induction of GAL4-dependent cDNA and dsRNA expression, progenies carrying GAL4 driver and UAS transgenes were raised at 28°C.

2.2. Transformation

To establish transgenic lines expressing nuclear-localized Cyclin B, *pUAS-CycB.HA-NLS* plasmid DNA was provided by F. Sprenger (Universität Regensburg, Regensburg, Germany) (Diennemann and Sprenger, 2004). Purified plasmid DNA was injected into *Drosophila* embryos via PhiC31integrase-mediated germ line transformation by using *Drosophila* Embryo Injection Services of the BestGene Inc. (Chino Hills, CA, USA).

2.3. Preparation of post meiotic spermatids

For the assessment of meiotic defects, we used the previously described protocol (Okazaki *et al*., 2020). A pair of testes collected from pharate adult or newly eclosed adult flies (0-2-day olds) were

 doi:10.20944/preprints202310.0751.v1

dissected in Testis buffer (183 mM KCl, 47 mM NaCl, 10 mM EDTA, pH 6.8) and covered with 18 x 18 mm-coverslip (Matsunami, Osaka, Japan) to flatten the cysts. To observe fixed post-meiotic spermatids, we removed the coverslips after freezing the slides and exposed slides to 100% methanol for 5 minutes at -30°C. Then, the sample was rehydrated in 1 x PBS (137.0 mM NaCl, 2.7 mM KCl, 10.1 mM $Na_2HPO_4 \cdot 12H_2O$, 1.8 mM KH_2PO_4). The observation was performed on a phase-contrast and fluorescent microscope (IX81, Olympus, Tokyo, Japan) and images were captured with a CCD camera (Hamamatsu Photonics, Shizuoka, Japan). Image acquisition was controlled through the Metamorph (Molecular Device, Sunnyvale, CA, USA) software.

2.4. Immunofluorescence

Testis cells were fixed according to the protocol described above. They were fixed with 100% ethanol for 10 minutes and with 3.7% formaldehyde for 7 minutes. The slides were permeabilized in PBST (PBS containing 0.01% Triton-X) for 10 minutes and blocked with 10% normal goat serum (Wako, Osaka, Japan) in PBS. Following primary antibodies were used at the dilution described; Rabbit anti-CycB antibody (Whitfield *et al*., 1990, a gift from D. Glover, Cambridge University, UK): 1/400, Mouse anti-HA (6E2, Cell signaling Technology, Danvers, MA, USA): 1/200, Mouse anti-MPM-2 antibody (05-368, Sigma-Aldrich, St, Louis, USA): 1/400, Guinea pig anti-Asl (Novak et al., 2014; a gift of J. Raff, University of Oxford, Oxford, UK): 1/800, Mouse anti-Cdk7 antibody (20H5, Developmental Studies Hybridoma Bank, Iowa University, Iowa, USA): 1/200, Rat anti-Twine antibody (Di Talia *et al*., 2013, a gift from E. Wieschaus, Princeton University, Princeton, USA): 1/100), Rabbit anti-Cdk1 antibody (06-923, Sigma-Aldrich, St, Louis, USA): 1/200, and Mouse anti-GFP antibody (3E6, Invitrogen, Carlsbad, CA, USA): 1/200. After incubating with the primary antibodies overnight at 4°C, the samples were washed in PBS and subsequently incubated with Goat anti-Mouse, Rabbit, or Rat IgG (H+L) conjugated with Alexa Fluor 488, 555 or 647 (Invitrogen, Carlsbad, CA, USA) for 2 hours at room temperature. After washing in PBS, the samples were mounted with VECTASHIELD Mounting Medium with DAPI. Image acquisition was performed described above.

2.5. Live cell imaging of primary spermatocytes

To observe the nuclear-cytoplasmic transport of CycB-GFP protein in living primary spermatocytes, we performed the time-lapse observation previously describe (Tanabe *et al*., 2019). A pair of testes collected from pharate adults were dissected in BRB80 buffer (80 mM PIPES, 1 mM $MgCl_2$, 1 mM EGTA, pH 6.8) under mineral oil (Trinity Biotech, Bray, Ireland) on a clean coverslip. To facilitate the observation of the nuclear import of CycB-GFP, we inhibited the exportin by Leptomycin B (Cayman Chemical, Michigan, USA). The drug was added to BRB80 buffer to a final concentration of 10μM. GFP fluorescence images were captured at each 60 seconds interval.

2.6. In situ proximity ligation assay (PLA)

We performed the PLA method to detect close interaction between Cdk1 and its positive regulators by using the Duolink kit (Sigma-Aldrich, St, Louis, USA) as described (Okazaki *et al*., 2020). We used the following combination of antibodies; Mouse anti-Cdk7 and Rabbit anti-Cdk1 antibodies to detect the complex containing Cdk7 and Cdk7; Mouse anti-GFP and Rabbit anti-Cdk1 antibodies to detect the complex containing Twine-GFP and Cdk1. Image acquisition was performed as described above.

3. Results

3.1. Continuous nuclear import and export of CycB via the Nup62 subcomplex in the nuclear pores during the growth phase of Drosophila spermatocytes before meiosis

CycB remains to be accumulated in the nucleus during the early stages of spermatocytes before meiosis, if the Nup62 subcomplex in the NPC or a *Drosophila* exportin orthologue is depleted; thereby, Cdk1 is not activated, and meiosis does not initiate (Okazaki et al., 2020). In this study, we first

Preprints (www.preprints.org) | NOT PEER-REVIEWED | Posted: 12 October 2023 doi:10.20944/preprints202310.0751.v1

performed immunostaining for CycB of spermatocytes and observed the cellular localization at S3–S6 in the growth phase and prophase I (ProI) (Figure 1A′ to E′). We determined the stages of spermatocytes according to the nucleolar size and morphology visualized using Spermatocyte arrest (Sa)-GFP (Azuma et al., 2019) (Figure 1A″ to E″). To investigate the cellular localization of CycB, we quantified fluorescence of CycB in the nucleus and cytoplasm. During S3–S5, we observed a weak fluorescence signal in the nucleus and cytoplasm. Thereafter, cytoplasmic localization became clear, and an intense signal was observed in the cytoplasm at S6 stage. After Sa-GFP fluorescence indicated disappearance of the nucleolus, CycB entered the nucleus (Figure 1E′). We quantitated mean fluorescence intensity in spermatocytes in each developmental stage (Figure 1F). CycB fluorescence in cells increased from S3 to S5 stage, and subsequently it increased more sharply from S5 to S6 stage, just before the onset of meiosis, although the ratio of nuclear to cytoplasmic (N/C) fluorescence was almost constant. CycB fluorescence continued to increase from S6 to ProI. To verify CycB dynamics, we next performed a time-lapse observation of GFP-tagged CycB in living spermatocytes (Figure 1 G, H, and I). Under drug-free *ex vivo* culture conditions, CycB in premeiotic spermatocytes was mostly localized in the cytoplasm and nucleolus (Figure 1G). However, in the presence of leptomycin B (LMB) that inhibited nuclear export, CycB was gradually accumulated in the nucleus, while GFP-CycB fluorescence in the nucleolus did not change (Figure 1H). The GFP fluorescence intensities of the nucleus and cytoplasm became almost equal after 70 min. The apparent lack of change in GFP fluorescence without the drug was owing to the balance between nuclear entry and export. Inhibition of nuclear export by LMB highlighted continuous nuclear export of CycB before meiosis. Therefore, a previous result that CycB is accumulated in the nucleus of *Nup62*-silenced spermatocyte is considered as a consequence of the disruption of nuclear export, and nuclear accumulation of CycB results in a failure of Cdk1 activation or meiosis initiation (Okazaki et al., 2020, Figure S1D, E).

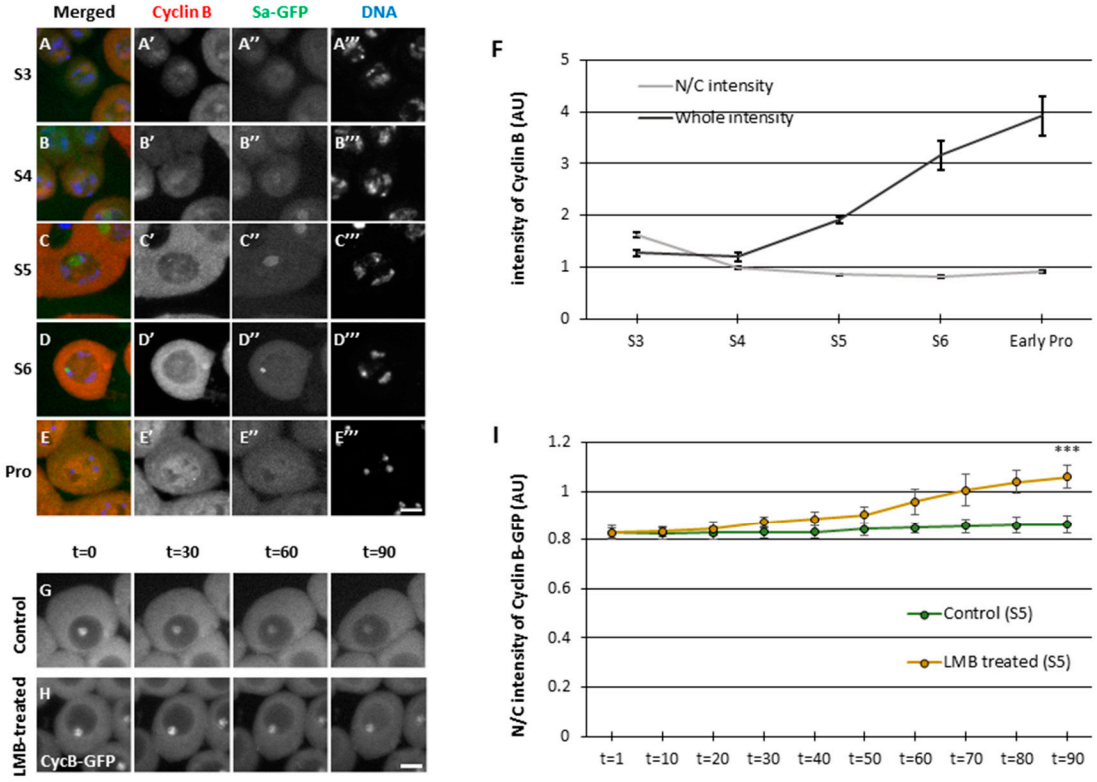

Figure 1. Nuclear–cytoplasmic shuttling of cyclin B in spermatocytes during the growth-phase. (A–E) Immunostaining of spermatocytes with anti-cyclin B (CycB) antibody from the growth-phase (S3-S6 in A–D) to the onset of meiosis [prophase I (ProI) in E]. Images show CycB immunofluorescence (red in A–E, white in A′–E′), Sa-GFP fluorescence for visualizing the nucleolus (green in A–E, white in A″–E″), and DNA staining with 4′,6-diamidino-2-phenylindole (DAPI) (blue in A–E, white in A‴–E‴). Scale bar, 10 μm (F) Quantification of CycB immunofluorescence intensity in whole

 doi:10.20944/preprints202310.0751.v1

spermatocytes (black line) and the nucleus, relative to that in the cytoplasm of spermatocytes (gray line) at each stage represented in A–E. Data represent mean ± 95% confidence interval (CI) (>16 cells). (G, H) Time-laps observation of CycB in the growth phase (S5) of living spermatocytes expressing CycB-GFP and treated with leptomycin B (LMB) (H) and that of untreated cells (G). Ninety images were captured every minute. Four selected images of a live spermatocyte are presented. Scale bar, 10 μm. (I) Comparative quantification of nuclear fluorescent intensity of GFP relative to that in the cytoplasmic fluorescent intensity in LMB-treated (orange line) and untreated (green line) spermatocytes expressing CycB-GFP. Data represent mean ± 95% Confidence Interval (CI) (11 untreated and eight LMB-treated spermatocytes). Significance was tested at the last time point (t = 90). $^{**}p < 0.001$ [one-way analysis of variance (ANOVA) followed by Bonferroni's post-hoc comparison].

3.2. Overexpression of normal CycB, but not CycB harboring nuclear localization signal (NLS), rescued inhibition of meiotic initiation in Nup62-depleted spermatocytes

We addressed the mechanism, by which the inhibition of nuclear export of CycB via an exportin orthologue and Nup62 inhibited Cdk1 activation. We analyzed whether the persistent accumulation of CycB, which could not be exported owing to *Nup62* silencing, in the nucleus is responsible for the failure of meiotic initiation. CycB carrying NLS (*bam>CycB-NLS*) or normal CycB (*bam>CycB*) (Figures S1F-H and 2A) was induced in spermatocytes (Figure S1L-N). CycB abundance was lower in the nucleus than in the cytoplasm of the control cells (*bam>+*). Ectopic expression of normal CycB in control cells did not significantly change its localization, whereas that of NLS-CycB increased the N/C ratio by 0.4 (Figure 2A). This indicates that NLS-CycB was accumulated in the nucleus. In contrast, the ratio significantly increased as a consequence of abnormal nuclear accumulation of CycB in the *Nup62*-silenced cells. Cytoplasmic CycB increased by ectopic expression of normal CycB in *Nup62*-silenced cells (*bam>CycB, Nup62RNAi*). In contrast, ectopic expression of NLS-CycB had no impact on the N/C ratio in *Nup62*-silenced cells (Figure 2A).

To investigate whether this change in the N/C ratio of CycB affects the initiation of meiosis, we observed the cysts of spermatids at the onion stage immediately after the completion of meiosis II. Sixteen premeiotic spermatocytes consisting of the cyst undergo two consecutive meiotic divisions synchronously. Eventually, a cyst consisting of 64 spermatids is generated after the second meiotic division. Each spermatid at the onion stage contains a single haploid nucleus and a single round-shaped mitochondrial derivative called Nebenkern. If the spermatocytes do not undergo meiotic divisions, resultant spermatid cysts consist of 16 cells only. Therefore, we can determine the occurrence of meiotic divisions by counting the number of cells contained in single spermatid cyst. In testes with *Nup62*-silenced spermatocytes (*bam>Nup62RNAi*), all spermatid cysts consisted of 16 cells (n = 24), while every spermatid cyst contained 64 post-meiotic cells in the control testes (n = 39) (Figure 2B). Every cell in the abnormal cysts possessed a bigger than normal nucleus. This phenotype of spermatids derived from the *Nup62*-silenced spermatocytes indicates that the spermatid cysts consisting of 16 cells resulted from a failure of two meiotic divisions. All spermatid cysts comprised 64 cells in *bam>CycB* (n = 15) or *bam>CycB-NLS* (n = 18) testes. Interestingly, overexpression of CycB in *Nup62*-silenced cells resulted in the generation of post-meiotic cysts consisting of 32 cells (12.5% of total spermatid cysts examined, 4 out of 32) and 64-cell cysts [56.2 % of the spermatid cysts (18/32)], while ectopic overexpression of NLS-CycB produced cysts containing 16 spermatids only (n = 24) (Figure 2B). Therefore, inhibition of meiotic initiation in *Nup62*-silenced spermatocytes was rescued by overexpression of CycB, but not NLS-CycB, suggesting that reduced cytoplasmic CycB, rather than the accumulation of ectopic nuclear CycB, inhibited meiotic initiation.

Preprints (www.preprints.org) | NOT PEER-REVIEWED | Posted: 12 October 2023 doi:10.20944/preprints202310.0751.v1

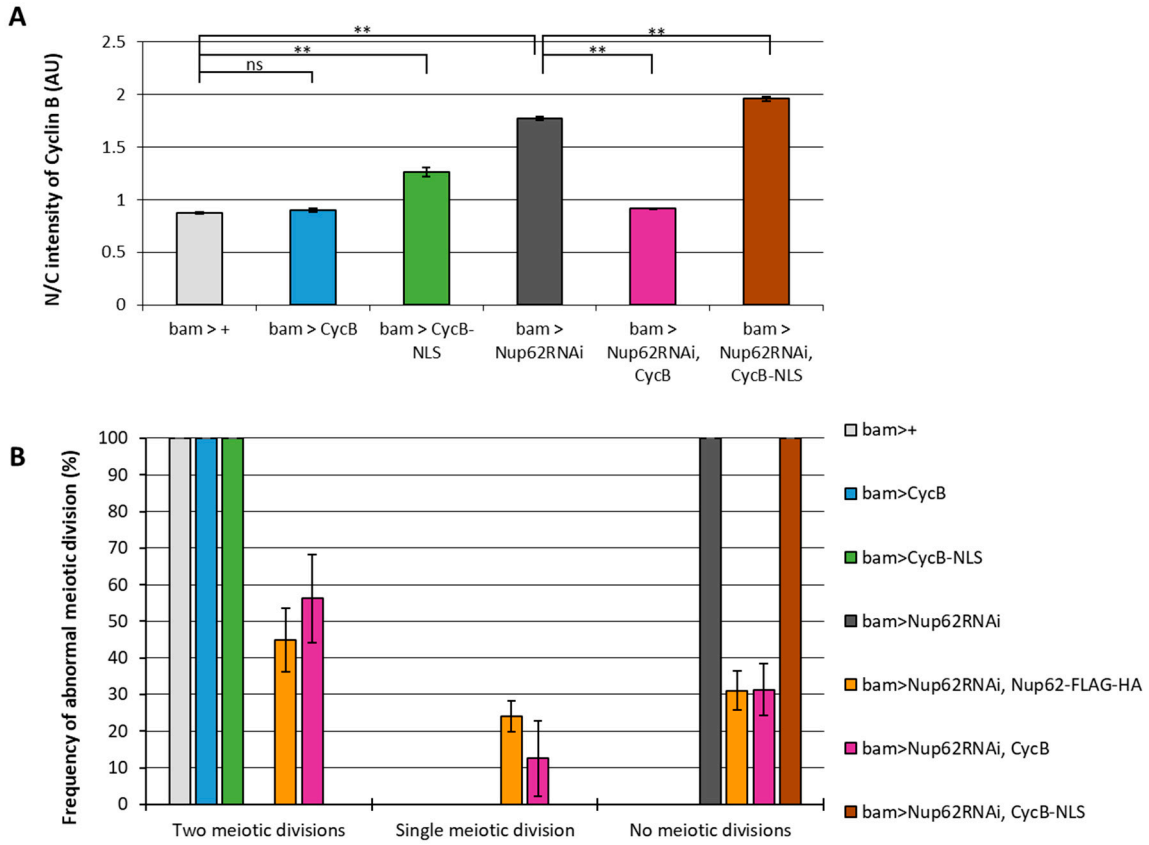

Figure 2. The effect of cytoplasmic CycB on the meiotic defect of Nup62-depleted spermatocytes (A) Quantification of the anti-CycB immunofluorescence intensity in the nucleus relative to the cytoplasm of growth phase spermatocytes (S5) of following genotypes; *bam* > + (light grey column), *bam* > *CycB* (blue column), *bam* > *CycB-NLS* (green column), *bam* > *Nup62RNAi* (dark grey column), *bam* > *Nup62RNAi, CycB* (magenta column), *bam* > *Nup62RNAi, CycB-NLS* (brown column). Data are presented as mean ± SEM (n > 15). one-way ANOVA followed by Bonferroni's post-hoc comparison. ** $p < 0.01$. n.s. not significant. (B) Frequency of spermatids cyst formed through two meiotic divisions (normal), single meiotic division (abnormal), or no meiotic divisions (abnormal). More than 60 spermatids cysts were collected from each of 36 testes of genotypes referred to in A in addition to another control, *bam* > *Nup62RNAi, Nup62* (orange column). Data are presented as mean ± SEM (n > 46).

3.3. Reduced activation of Cdk1 during the growth phase and its full-scale activation immediately after rapid reentry of CycB into the nucleus at the onset of meiosis

To further analyze the relationship between Cdk1 activity and CycB localization before and at the onset of meiosis, we performed simultaneous immunostaining with the anti-mitotic protein monoclonal 2 (MPM2) antibody that can recognize the epitopes phosphorylated by several kinases including CDK1 (Okazaki et al., 2020). In normal spermatocytes at S5 stage (*bam*>+), faint MPM2 fluorescent signal colocalized with Sa-GFP foci in the nucleolus (Figure 3A, A'). A subtle CycB signal was observed in the cytoplasm at S5 (Figure 3A, A''). With the shrinkage of the nucleolus visualized by Sa-GFP (Figure 3B, B''') associated with phosphorylation of nucleolar proteins by CDK, MPM2 signal over a detectable level was not observed (Figure 3B, B'). CycB signal in the cytoplasm became slightly more intense at S6, although the N/C ratio of CycB immunofluorescence intensity did not significantly increase ($p = 0.93$) (Figure 3B, E). In cells showing condensed chromosomes at ProI (Figure 3C''''), the N/C ratio slightly increased ($p < 0.01$), indicating that CycB started entering the nucleus from the cytoplasm (Figure 3C'', E). When CycB signal was detected in the nucleus, MPM2 epitopes appeared in the nucleus (Figure 3C'). Subsequently, the signal intensity sharply increased in the nucleus and cytoplasm from early ProI to prometaphase I (Prometa) (Figure 3D, D''', E) ($p <$

Preprints (www.preprints.org) | NOT PEER-REVIEWED | Posted: 12 October 2023 doi:10.20944/preprints202310.0751.v1

0.01). These observations indicated that full-scale activation of CycB occurred at the nucleus after its rapid reentry, and it spread immediately to the cytoplasm from earlier ProI to PrometaI (Figure 3E), when Sa-GFP foci were no longer detected (Figure 3D‘’’)). The robust intensity of anti-MPM2 signal in *Nup62*-silenced cells has not been previously observed (Okazaki et al., 2020). Considering the importance of cytoplasmic CycB, we conclude that the full-scale activation of Cdk1 was suppressed in *Nup62*-silenced cells.

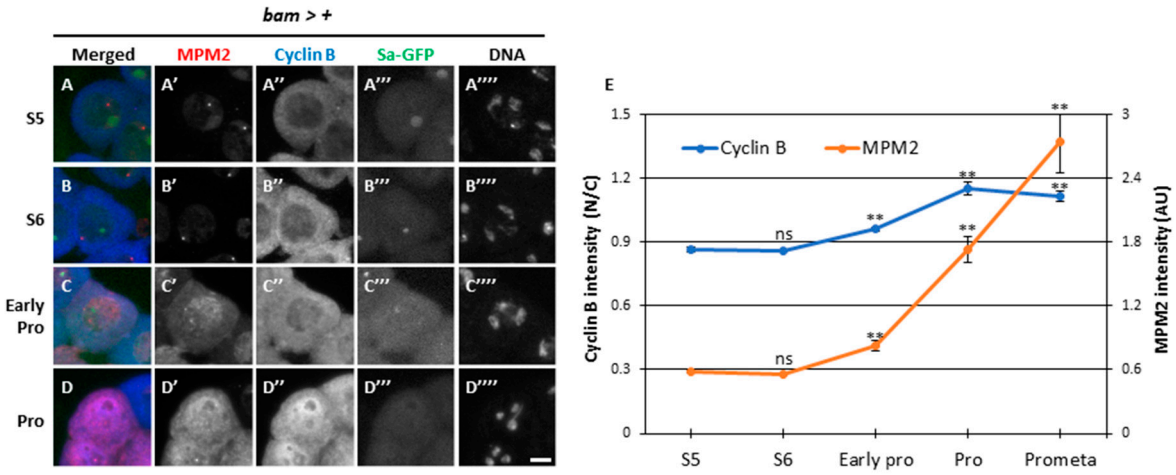

Figure 3. The timing of full-scale activation of Cdk1-CycB and nuclear re-entry of CycB in the onset of meiotic division. (A-D) Fluorescent images of mature spermatocytes co-immunostaining with anti-MPM2 and -CycB antibodies before (A and B) and immediately after the onset of meiosis (C) and during meiosis (D). Images show anti-MPM2 (red in A-D, white in A’-D’) and anti-CycB (blue in A-D, white in A’’-D’’) immunofluorescence, Sa-GFP fluorescence for visualizing the nucleolus (green in A-D, white in A’’’-D’’’), and DNA staining with DAPI (white in A’’’’-D’’’’). Scale bar: 10μm. (E) Quantification of anti-MPM2 and nuclear anti-CycB immunostaining intensity at each stage represented in A-D. Analysis was performed on 71 cells in the S5, 133 cells in the S6, 30 cells in the early Prophase, 24 cells in the Prophase, and 7 cells in the Prometaphase. Data are presented as mean ± SEM. Significance was tested by one-way ANOVA followed by Bonferroni’s post-hoc comparison tests. $^{**}p < 0.01$.

3.4. Centriole separation in the cytoplasm prior to full-scale activation of Cdk1 depended on Cdk1, which was not observed in Nup62-silenced spermatocytes

Initial activation triggers full-scale activation of Cdk1 in mitosis (Lindqvist, 2009). Although we detected faint signals for MPM2 epitopes at S5 and S6 stages, whether partial activity of Cdk1 was required for certain cellular events at the premeiotic stage was unclear. A pair of centrosomes separate from each other before ProI, which requires Cdk1 for separase activation. In control spermatocytes (*bam*>+), a pair of centrosomes was visualized by immunostaining for Asterless (Asl), which was localized next to each other at S5 stage (Figure 4A’). They separated from each other at S6 (Figure 4B’) and reached the opposite poles in cells at ProI (Figure 4C’). The distance between the two centrosomes significantly increased as the cells proceeded from S5 to S6 and then to ProI ($p < 0.01$) (Figure 4H). In contrast, centrosome separation was inhibited in spermatocytes harboring cell-specific *Cdk1RNAi* (Figure 4D, E, gray bars in 4H), although MPM2 epitopes were not seen on centrosomes (Figure 4A-C). Similarly, the separation was also inhibited in *Nup62*-silenced spermatocytes (Figure 4F, G, light gray bars in 4H). The mean distance between paired centrosomes at S5 did not significantly alter in *Cdk1*- or *Nup62*-silenced cells as that in the controls. As the control spermatocytes developed, the distance at S6 increased by 2-folds compared to that at S5 ($p < 0.01$) and further increased by 3-folds at ProI ($p < 0.01$). In contrast, the distance in *Nup62*-silenced cells at S6 did not significantly increase compared to that in cells harboring either of gene silencing (Figure 4H). Therefore, we concluded that centrosome separation before the onset of meiosis was disrupted in *Nup62*-silenced spermatocytes as in *Cdk1*-silenced cells. These phenotypes suggest that initial

Preprints (www.preprints.org) | NOT PEER-REVIEWED | Posted: 12 October 2023 doi:10.20944/preprints202310.0751.v1

activation of Cdk1 at a low level was required for centrosome separation, and that this activity was inhibited in *Nup62*-silenced spermatocytes.

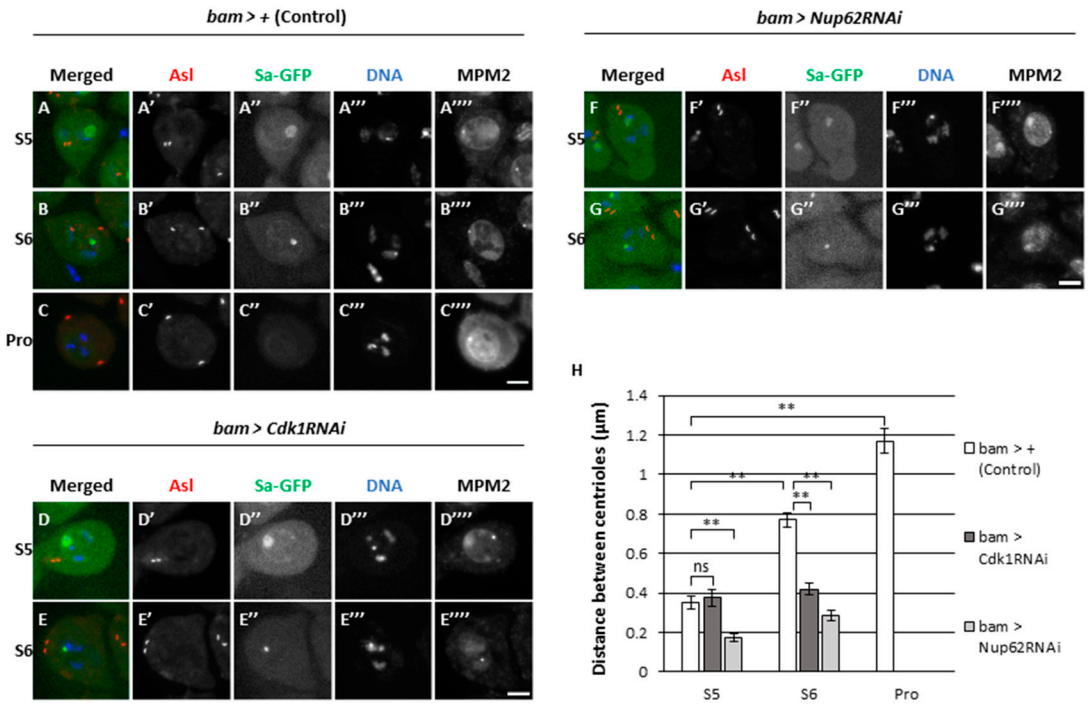

Figure 4. Cdk1-mediated centriole separation and nucleolus disassembly before the initiation of meiotic division.(A-G) Observation of mature spermatocytes (the growth phase at S5 and S6 in A, B, D-G, at prophase I (Pro in C) immunostaining with anti-Asl and anti-MPM2 antibodies. Normal control (*bam* > +) (A-C), *Cdk1*-silenced (D and E) and *Nup62*-silenced (F and G). Images show anti-Asl immunofluorescence to visualize centrosomes (blue in A-G, white in A'-G'), Sa-GFP fluorescence for visualizing the nucleolus (green in A-G, white in A''-G''), DNA staining with DAPI (white in A'''-G''') and anti-MPM2 epitopes (red in A-G, white in A''''-G''''). Scale bar: 10μm. (H) Quantification of distance between paired centrosomes at S5 to ProI spermatocytes. Normal control cells (white columns), *Cdk1*-silenced (dark grey columns), and *Nup62*-silenced (dark grey column) spermatocytes. Data are presented as mean ± SEM (n > 29 cells). No ProI cells were observed in *bam>Cdk1RNAi* or *bam>Nup62RNAi* testes. Significance was tested by one-way ANOVA followed by Bonferroni's post-hoc comparisons tests. ** $p < 0.01$.

3.5. A close association of Cdk1 with its activator CAK was observed in the nucleus during the growth phase in both normal and Nup62-silenced spermatocytes before meiosis

Next, we analyzed why Cdk1 was not activated even at a low level in *Nup62*-silenced spermatocytes (*bam>Nup62RNAi*). Three essential modifications are required for Cdk1 activation including association with the M-phase cyclin, CycB, phosphorylation of Cdk1 at Thr^{161} by CAK, and dephosphorylation of Cdk1 at Thr^{14} and Tyr^{15} by Twine phosphatase. We investigated the subcellular localization of CAK and assessed its close association with Cdk1. We performed immunostaining on control cells (*bam*>+) using anti-Cdk7 antibody which specifically recognizes the catalytic subunit of CAK (Figure 5A-C). Fluorescent signal was noticed in the nucleolus of spermatocytes at S5 and subsequently spread over the whole region of the nucleus at S6, and no signal was detected at ProI and thereafter (Figure 5A-C). To investigate whether Cdk1 was associated with CAK in spermatocytes, we performed Proximity Ligation Assay (PLA) *in situ* that can detect close association between two proteins if they are present in close proximity to form a complex. Fluorescent signal of Cdk7 was detected in the nucleus of normal cells at S5 and S6 stages (Figure 5A, B). Consistently, PLA signals were observed only in the nucleus at both stages (Figure 5G, H), suggesting that Cdk1

Preprints (www.preprints.org) | NOT PEER-REVIEWED | Posted: 12 October 2023 doi:10.20944/preprints202310.0751.v1

underwent phosphorylation by CAK in the nucleus. Similarly, both Cdk7 (Figure 5D, E) and PLA signals (Figure 5I, J) were specifically observed in the nucleus of *Nup62*-silenced cells at both stages, as observed in normal cells. These data confirmed that Cdk was normally phosphorylated by CAK in the nucleus of *Nup62*-silenced spermatocytes.

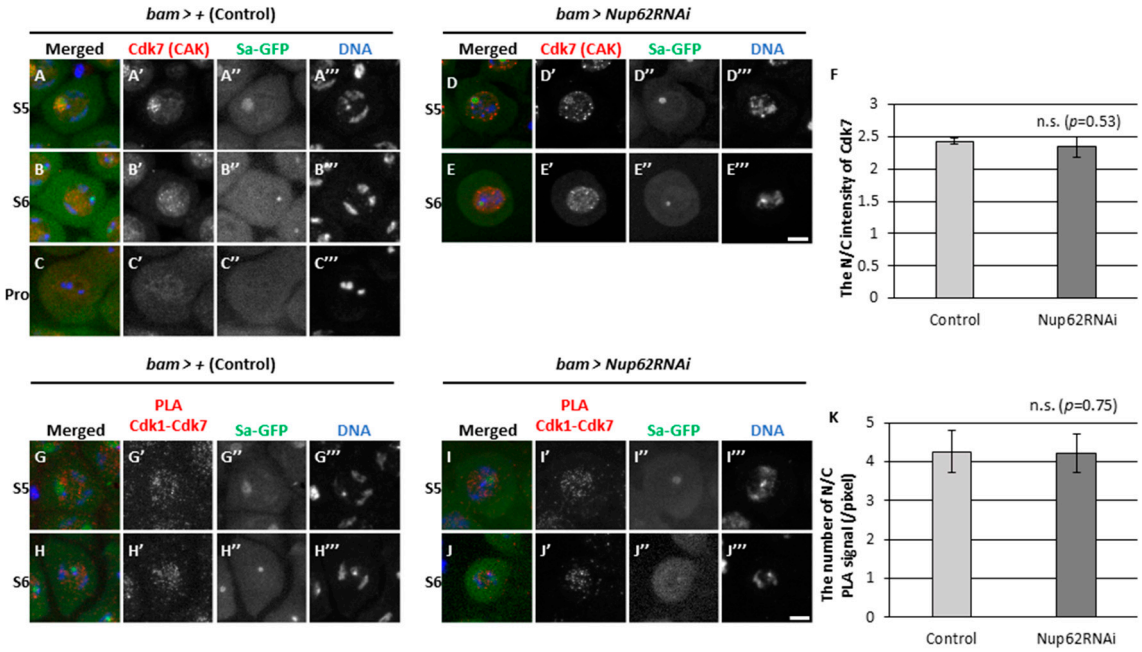

Figure 5. Intracellular localization of Cdk7 and PLA *in situ* analysis to monitor a close association between Cdk1 and Cdk7 in spermatocytes at S5, S6 and ProI.(A-E) Anti-Cdk7 immunostaining of normal (A-C) and *Nup62*-silenced (D and E) spermatocytes at growth phase (A, D at S5 and B, E at S6) and Prophase (Pro) (C). Images show anti-Cdk7 immunofluorescence (red in A-E, white in A'-E'), Sa-GFP fluorescence for visualizing the nucleolus (green in A-E, white in A''-E''), and DNA staining with DAPI (blue in A-E, white A'''-E'''). Scale bar: 10μm. (F) Ratio of the intensity of anti-Cdk7 immunofluorescence in the nucleus over that in the cytoplasm. Data are presented as mean ± 95% CI (n >16 cells for each genotype). Significance was tested by Mann–Whitney test. n.s. ; not significant. (G-J) PLA *in situ* analysis to detect the close interaction between Cdk1 and Cdk7 in normal (G, H) and *Nup62*-silenced (I, J) spermatocytes at S5 (G, I) and S6 (H, J). Scale bar: 10μm. (K) Ratio of the number of PLA signals in the nucleus over that in the cytoplasm. Data are presented as mean ± 95%CI (n > 300 cells). Significance was tested by Mann–Whitney test.

3.6. The association of Cdk1 with its activator phosphatase Twine in the nucleus and cytoplasm before meiosis did not change in Nup62-silenced cells

Next, we assessed if dephosphorylation of Cdk1 at Thr^{14} and Tyr^{15} by Twine phosphatase occurred in *Nup62*-silenced spermatocytes. As specific antibodies against phosphorylated Thr^{14} and Tyr^{15} of *Drosophila* Cdk1 were not available, we performed immunostaining using anti-Twine antibody to detect its cellular localization before meiosis and subsequently examined its association with Cdk1. We performed immunostaining of control cells (*bam*>+) at S3 to ProI with anti-Twine (Figure 6A-E). Weak fluorescent signal was noticed in the nucleus and cytoplasm of spermatocytes at S3 and S4 (Figure 6A, B), and distinctive signals were predominantly observed in the nucleus from S5 to ProI (Figure 6C-E, 6C'-E'). Similarly, fluorescent signal was detected in the nucleus of Nup62-silenced spermatocytes at S5 and S6 (Figure 6F-I). The N/C ratio of fluorescence intensity was > 1.0, suggesting that more Twine was localized in the nucleus. We next performed *in situ* PLA assay to detect complex formation between Cdk1 and Twine before meiosis. PLA signals were observed in normal spermatocytes at S5 and S6 (Figure 6K-M), indicating that Cdk1 may undergo dephosphorylation by Twine in the nucleus and cytoplasm. Additionally, PLA signals were observed

Preprints (www.preprints.org) | NOT PEER-REVIEWED | Posted: 12 October 2023 doi:10.20944/preprints202310.0751.v1

in Nup62-silenced cells at S5 and S6 (Figure 6N, O). These data suggested that Cdk activation by Twine can take place in whole regions of normal and Nup62-silenced cells.

We observed fluorescence of Wee1-GFP (Figure S2A′-C′) and Myt1-GFP (Figure S2D′-F′) predominantly in the nucleus and cytoplasm at S5 and S6 and during ProI. PLA assay detected complexes containing Wee1-GFP and Cdk1(Figure S2G′, H′) and Myt1-GFP and Cdk1(Figure S2I′, J′) in the nucleus and cytoplasm before meiosis and ProI. Based on these results, we concluded that Wee1/Myt1 kinases may be associated with Cdk1 during S5–ProI. Next, we investigated whether Polo, an indispensable protein kinase that controls the G2/M transition of the mitotic cycle is required for meiotic initiation. We noticed many spermatid cysts consisting of 16 cells harboring multiple nuclei, suggesting that chromosome segregation took place but cytokinesis did not occur in either of the meiotic divisions (Figure S3A). Consistently, even in *polo*-silenced spermatocytes, MPM2 epitopes appeared from S6 to ProI, as observed in control spermatocytes (Figure S3B′-D′). Immunofluorescence staining indicated that Polo migrated into the nucleus slightly earlier than did CycB (Figure S4C″-E″). Similarly, Polo was localized in the cytoplasm at and before S6 in *Nup62*-silenced cells, whereas CycB was not exported from the nucleus (Figure S4G′, H′). No detectable differences in the subcellular localization of Polo were noticed in *Nup62*-silenced cells. Moreover, PLA signals indicated complex formation between CycB and Polo-GFP in the nucleus and cytoplasm of control (*bam*>+) (Figure S5A′-C′) and *Nup62*-silenced cells (Figure S5D′, E′).

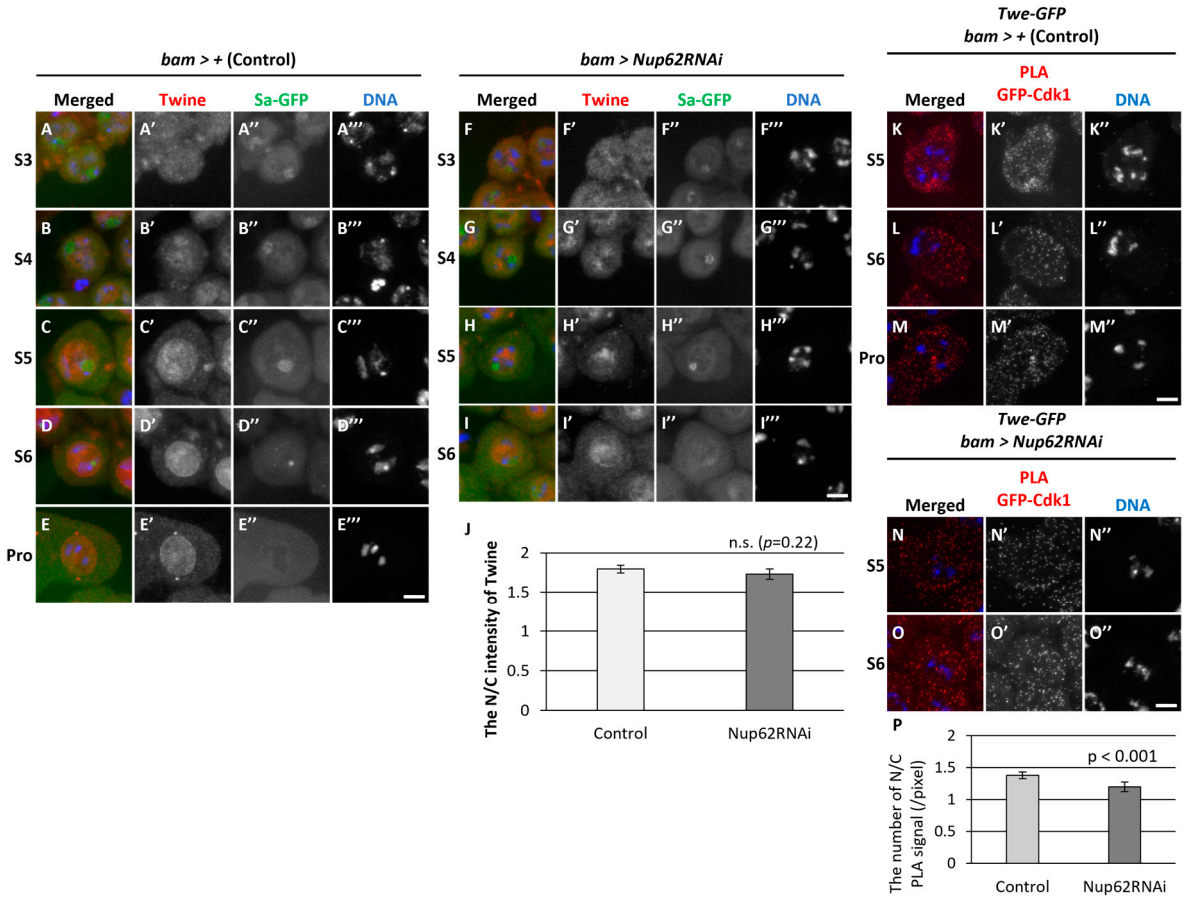

Figure 6. Intracellular localization of Twine and PLA *in situ* analysis to monitor a close association between Cdk1 and Twine. (A-I) Anti-Twine immunostaining of normal (A-E) and *Nup62*-depleted (F-I) spermatocytes at S3 to S6 of the growth phase (A-E, and F-I) and prophase I (Pro) (E). Images show anti-Twine immunofluorescence (red in A-I, white in A′-I′), Sa-GFP fluorescence for visualizing the nucleolus (green in A-I, white in A″-I″), and DNA staining with DAPI (blue in A-I, white A‴-I‴). Scale bar: 10μm. (J) Ratio of the intensity of anti-Twine immunofluorescence in the nucleus over that in the cytoplasm. Data are presented as mean ± 95% CI (n > 18 cells). Significance was tested by Mann–Whitney test. *** $p < 0.001$. (K-O) PLA *in situ* analysis to detect the close interaction between in

 doi:10.20944/preprints202310.0751.v1

normal (K-M) and *Nup62*-silenced (N, O) spermatocytes at pre-meiotic stage (K, N at S5 and L, O at S6) and prophase I (Pro)(M). Scale bar: 10μm. (P) Ratio of the number of PLA signals in the nucleus over that in the cytoplasm. Data are presented as mean ± 95%CI (n > 300 cells). Significance was tested by Mann–Whitney test.

3.7. Simultaneous silencing of the Cdk inhibitor, Rrouhex (Rux), but not Z600, rescued the inhibition of meiotic initiation by silencing of Nup62

Cdk1 was not activated in the spermatocytes before initiation of meiosis if CycB was accumulated in the nucleus owing to the inhibition of nuclear export. No remarkable differences in the association of CAK or Twine with Cdk1 were observed between normal and *Nup62*-silenced cells. Unlike overexpressed CycB, ectopic expression of constitutively active Cdk1 ($Cdk1^{T14AY15F}$) cannot reverse the inhibition of meiotic initiation in *Nup62*-silenced cells (Okazaki et al., 2020); therefore, we hypothesized that a negative regulator represses Cdk1 activity in the nucleus independent of Cdk1 modification. We investigated whether another type of inhibitor different from Wee1/Myt1 is involved in regulating Cdk1 before meiosis. Two Cdk inhibitors (CKIs), Z600/Frs and Rux, bind to CycB–Cdk1 (Foley et al., 1999, Gawlinski, et al., 2007). Immunostaining of the spermatocytes in normal testes (*bam*>+) using anti-Z600 antibody and observation of spermatocytes expressing HA-tagged Z600 revealed that Z600 was localized in the nucleus of spermatocytes at S5 and ProI (Figure S6A′, C′). At S6 stage, distinct fluorescent signal was predominantly observed in the nucleus, with less intense signal in the cytoplasm (Figure S6B′). These signals were almost lost in *Z600*-silenced spermatocytes (Figure S6D′, E′). However, Z600 depletion did not influence the meiotic phenotype of *Nup62*-silenced cells. Rux is a negative regulator of the CycA–Cdk1 complex; however, it can bind to CycB–Cdk1 to suppress its kinase activity (Foley et al., 1999). We investigated whether Rux is involved in repressing Cdk before meiosis. In testes harboring *Nup62*-silenced spermatocytes, all spermatid cysts (n=39 cysts) consisted of 16 cells (Figure 7B). In contrast, testes harboring the *rux*-silenced spermatocytes contained abnormal spermatid cysts. Although they consisted of 64 spermatids, 59 out of 70 cells harbored small and multiple nuclei (Figure 7C). This meiotic phenotype was consistent with the reported phenotype of hypomorphic *rux* mutants that originated because of an extra round of chromosome segregation without cytokinesis (Gonczy, et al., 1994). In testes containing spermatocytes harboring simultaneous silencing of *Nup62* and *rux* (*bam>Nup62RNAi, ruxRNAi*), we frequently observed spermatid cysts consisting of 16 cells, some of which contained multiple small nuclei (arrow in Figure 7D), indicating that chromosome segregation occurred without cytokinesis (100/109 cells). Other spermatids contained nuclei larger than those of normal spermatids, indicating that meiosis did not occur as shown in spermatid cysts of *Nup62*-silenced testes (arrowhead in Figure 7D) (9/109 cells). These phenotypes suggested that *rux* silencing rescued the inhibition of meiotic initiation in *Nup62*-silenced spermatocytes. Consistent with this finding, we observed several spermatocytes with intense MPM2 signals in the nucleus and cytoplasm of matured spermatocytes harboring *ruxRNAi and Nup62RNAi* (Figure 7I′, J) [10% (31/303 cells)]. Control cells (*bam*>+) also exhibited MPM2 epitopes at equivalent frequency. The number of MPM2-positive spermatocytes increased in testes harboring *rux*-silenced spermatocytes (46/87 cells). These results suggest that *rux* silencing can rescue meiotic cell cycle arrest in *Nup62*-silenced spermatocytes.

Preprints (www.preprints.org) | NOT PEER-REVIEWED | Posted: 12 October 2023 doi:10.20944/preprints202310.0751.v1

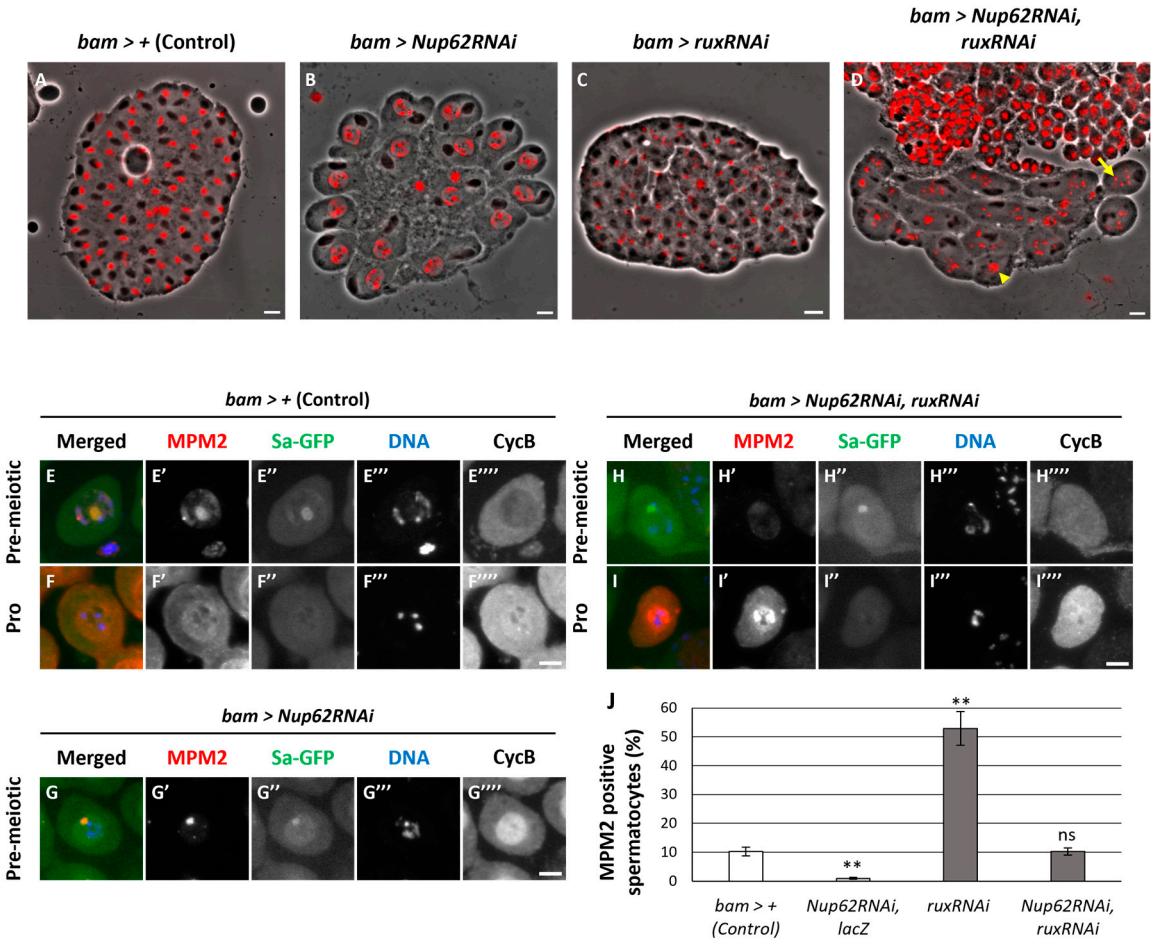

Figure 7. Rescue of the phenotypes of *Nup62RNAi* spermatocytes including a failure of meiotic divisions, the loss of anti-MPM2 immunostaining in the cytoplasm and nucleus and the nuclear accumulation of CycB by simultaneous depletion of *rux* encoding a CKI. (A-D) Phase contrast micrographs of a single intact cyst composed of spermatids at the onion stage after the completion of meiosis II or a slightly later stage. (A) A normal control spermatid cyst contained 64 cells. (B) an intact spermatid cyst composed of 16 spermatids derived from *Nup62RNAi* spermatocytes without meiotic divisions. The spermatids harbor under-condensed chromatin in the nuclei. (C) an intact spermatid cyst containing > 64 nuclei with smaller size and > 64 Nebenkerns generated from *ruxRNAi* spermatocytes. (D) an intact-like spermatid cyst containing > 16 Nebenkerns and multiple smaller nuclei (arrow) together with larger-sized nuclei (arrowhead), which were derived from spermatocytes harboring *Nup62RNAi* and *ruxRNAi*, suggesting meiotic divisions occurred in some spermatocytes of the cyst. Nuclei stained with DAPI are colored in red. Black round-shaped or slightly extended black structures adjacent to nuclei correspond to Nebenkern, a mitochondrial derivative. Bar: 10 μm. (E-G) Anti-MPM2 immunostaining (red in E-G, white in E'-G') of spermatocytes at premeiotic S5 or earlier stages to monitor the Cdk1 activation. Sa-GFP (green in E-G, white in E''-G'') is a marker to identify the stage of the growth phase. DNA staining (blue in E-G, white in E'''-G'''). Anti-CycB immunostaining (white in E''''-G''''). Bar: 10 μm. (E, F) control spermatocytes at the premeiotic stage (E) and ProI (F). (G) Spermatocytes harboring testis-specific depletion of *Nup62* (*bam>Nup62RNAi*) at the premeiotic stage (E) and ProI (F). (H, I) Spermatocytes harboring testis-specific simultaneous depletion of *Nup62* and *rux* (*bam>Nup62RNAi, ruxRNAi*) at premeiotic (H) and ProI (I). Stages of spermatocytes was determined using Sa-GFP marker. (J) Frequencies of spermatocytes harboring MPM2 epitopes of control (*bam>+*), *Nup62RNAi* (*bam>Nup62RNAi, LacZ*), *ruxRNAi* (*bam>ruxRNAi*), and *Nup62RNAi* and *ruxRNAi* (*bam>Nup62RNAi, ruxRNAi*) spermatocytes. ** $p < 0.01$, n.s. not significant. one-way ANOVA followed by Bonferroni's post-hoc comparison. Error bars indicate SEM.

Preprints (www.preprints.org) | NOT PEER-REVIEWED | Posted: 12 October 2023 doi:10.20944/preprints202310.0751.v1

3.8. Depletion of importin β inhibited rapid nuclear reentry of CycB and initiation of meiosis but did not affect centrosome separation before meiosis

When nuclear import of CycB in the premeiotic spermatocytes treated with LMB, the protein was more rapidly imported to the nucleus at the onset of meiosis. It took over an hour for CycB in the nucleus and cytoplasm to become almost equal (Figure 1I). By contrast, it took only 6 to 7 minutes at the onset of meiosis (Figure 8A, B). To identify the factors required for the rapid nuclear import of CycB at the onset of meiosis, we investigated whether any nucleocytoplasmic transport receptor that imports and exports proteins through the nuclear pores was involved in the nuclear import of CycB. We silenced *Fs(2)Ket* encoding *Drosophila* importin β by RNAi . Spermatocyte-specific silencing of importin β revealed that all spermatid cysts at the onion stage (12/12 cysts) consisted of 16 cells, in which three clusters of condensed chromosomes were still observed (Figure S7D). The chromatin organization in the spermatids was different from that in *Nup62*- or *emb*-silenced spermatids, in which under-condensed chromatin was present in the nucleus (Figure S7B, C). Therefore, meiotic initiation was inhibited in *Fs(2)Ket*-silenced spermatocytes, and the cell cycle was arrested at different stages immediately before full-scale activation of Cdk1. To clarify this, we investigated the cellular localization of CycB. In control testes (*bam*>+), we observed robust CycB-GFP fluorescence in the cytoplasm of spermatocytes at S5 stage; however, no fluorescence was noticed in the nucleus of spermatids at the onion stage (Figure 8C′, D′). CycB-GFP fluorescence was observed in the nuclei of *Nup62*-silenced spermatocytes (*bam*>*Nup62RNAi*) at the same stage (Figure 8E′), and fluorescent signal sustained in the nucleus of spermatids harboring Nebenkerns (arrow in Figure 8F). In contrast, CycB-GFP was localized in the cytoplasm of *Fs(2)Ket*-depleted cells (Figure 8G′, H′). These cytological phenotypes and cellular localization of CycB are consistent with the interpretation that *Fs(2)Ket* is required for nuclear import of CycB–Cdk1 to complete full-scale activation of Cdk1. *Fs(2)Ket*-depletion did not influence centrosome separation, which is required for initial activation of Cdk1 before meiosis (Figure 8K, L, M). Unlike that in *Cdk1*- or *Nup62*-silenced cells (Figure 4D′-G′), centrosome separation in *Fs(2)Ket*-silenced spermatocytes was indistinguishable from that of the control cells (Figure 8I′-L′). Therefore, centrosome separation was not affected by inhibition of reentry of CycB into the nucleus.

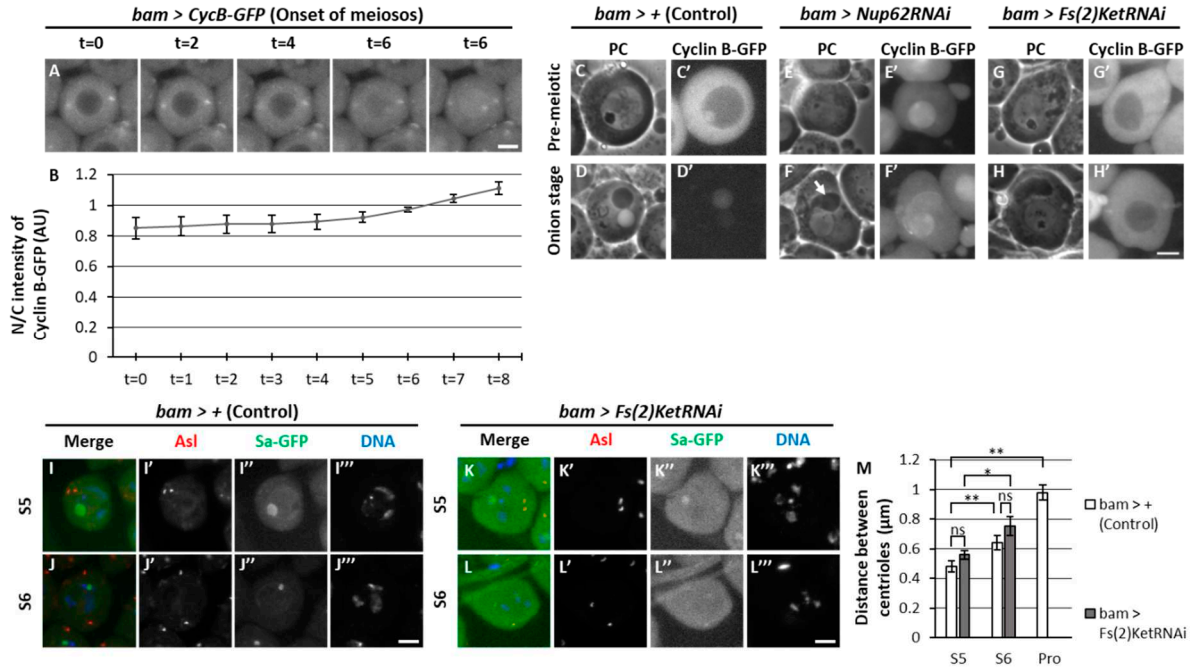

Figure 8. Silencing of *Fs(2)Ket* resulted in the failure of meiotic divisions in spermatocytes and subsequent spermatid differentiation without meiosis. (A) Time-laps observation of GFP-CycB fluorescence in live mature spermatocytes at onset of meiosis. Ten images were captured every minute from the timepoint when a pair of centrosomes reached opposite poles (t = 0). Four selected

Preprints (www.preprints.org) | NOT PEER-REVIEWED | Posted: 12 October 2023 doi:10.20944/preprints202310.0751.v1

images of a live spermatocyte are presented. Scale bar, 10 μm. (B) Quantification of nuclear fluorescent intensity of GFP relative to that in the cytoplasm of spermatocytes. Data represent mean ± 95% CI (10 spermatocytes). (C–H) Fluorescence micrographs of living spermatocytes or spermatids. (C′–H′) CycB-GFP fluorescence in premeiotic spermatocytes harboring nucleoli (C, E, G) and onion-stage spermatids (D, F, H). Relatively dark spheres in phase contrast micrographs of spermatocytes correspond to the nucleolus. A white or less dark sphere and darker round or ellipsoid-shaped spheres represent the nucleus and Nebenkern, respectively. (C, D) Normal control cells (*bam*>+). (E, F) *Nup62RNAi* cells (*bam>Nup62RNAi*). (G, H) *Fs(2)KetRNAi* cells (*bam>Fs(2)RNAi*). Growth stages of cells were determined according to the size and morphology of nucleolus. Scale bar, 10 μm. (G, H) control spermatocytes (*bam*>+) at S5 (G) and S6 (H). (I, J) Spermatocytes harboring *Fs(2)KetRNAi* (*bam>Fs(2)RNAi*) at S5 (K) and S6 (L). Growth stages were determined using Sa-GFP fluorescence. (M) Quantification of distance between paired centrosomes of spermatocytes at S5 to ProI. Control cells (white columns) and *Fs(2)Ket*-silenced [*bam>Fs(2)KetRNAi*, dark grey column] spermatocytes. Data are presented as mean ± standard error of the mean（SEM) (n > 38 cells). No ProI cells were observed in bam>*Fs(2)KetRNAi* testes. Significance was tested by one-way ANOVA followed by Bonferroni's post-hoc comparison. ** $p < 0.01$.

4. Discussion

4.1. Loss of cytoplasmic CycB and concomitantly reduced initial Cdk1 activity inhibits meiosis in Nup62-silenced spermatocytes where nuclear export is disrupted

Cdk1 activation is an essential step for initiating mitotic and meiotic divisions. Depletion of Nup62 subcomplex of NPC inhibits Cdk1 activation and meiotic initiation. CycB is accumulated in the nucleus of *Nup62*-silenced cells, whereas it was localized in the cytoplasm of normal cells before meiotic initiation (Okazaki *et al*., 2020). We assessed why CycB–Cdk1 was localized in the nucleus by downregulating Nup62 subcomplex or exportin orthologue. After the growth phase in normal spermatocytes, it migrated to the nucleus, and meiosis started. Based on these results, we speculated that abnormal subcellular localization may be involved in inhibiting Cdk1 activation in *Nup62*-silenced cells. CycB should be transported to the nucleus of spermatocytes in advance in early stages of the growth phase. Cyclin B1 continuously shuttles in and out of the nucleus before M-phase in human cells (Hagting, *et al*., 1999). Similarly, we observed that CycB was transported to the nucleus and then immediately exported from the nucleus during the growth phase in normal spermatocytes. Two reasons behind cell cycle arrest following *Nup62* silencing before initiation of meiosis may be considered as follows: (1) CycB–Cdk1 precociously localized in the nucleus as a consequence of *Nup62* silencing would dominantly inhibit the activation of endogenous Cdk1 before the onset of meiosis; (2) the reduced amount of Cdk1–CycB in the cytoplasm of *Nup62*-silenced cells would inhibit meiotic initiation. Ectopic overexpression of CycB, but not NLS-CycB, rescued the inhibition of meiotic initiation in *Nup62*-silenced cells. These observations support the second possibility that cytoplasmic CycB is more important than nuclear CycB for Cdk1 activation.

Absence of MPM2 epitopes in the nucleus and cytoplasm in the silenced cells indicated that Cdk1 was not activated in either compartment. Consistently, Cdk1-dependent events, such as centrosome separation, were suppressed in the cytoplasm, suggesting that initial Cdk1 activation takes place in the cytoplasm. Therefore, CycA–Cdk1 can be considered as a regulator of initial activation. *Drosophila* CycA functions as a mitotic cyclin, unlike its mammalian orthologue. It is translated earlier than CycB during the growth phase (White-Cooper *et al*., 1998). In spermatocytes expressing constitutively active Cdk1, which is not suppressed by Myt1, and *myt1* hypomorphic mutant cells, premature centriole disengagement occurs. This meiotic phenotype can be suppressed by the depletion of CycA activity (Varadarajan, *et al*., 2016). These previous results suggest that CycA–Cdk1 activity can influence centrosome dynamics in male meiosis. We have observed that a CycA depletion results in the accumulation of CycB in the nucleus during the G2 phase and inhibition of full-scale activation of Cdk1 (Tanaka, Y., Yamazoe, K. and Inoue, Y.H. unpublished). Further studies are necessary to clarify the possible role of CycA–Cdk1 in meiotic initiation.

 doi:10.20944/preprints202310.0751.v1

4.2. Cdk1 activation may be suppressed in the nucleus of spermatocytes by Roughex until onset of meiosis

Male meiosis does not initiate until Cdk1-CycB is exported from the nucleus to the cytoplasm during the growth phase. Inhibition of meiosis in *Nup62*-silenced spermatocytes is not responsible for perturbation of dephosphorylation of Tyr^{14} and Thr^{15} residues of Cdk1 by Twine as previously reported, or for that of phosphorylation of Thr^{161} by CAK in the present study (Okazaki *et al*., 2020). Therefore, mechanisms other than protein modification may suppress Cdk1 activation. CKIs directly bind to cyclin–Cdk complexes to suppress their activities and regulate cell cycle progression (Dash and El-Deiry, 2005). Our genetic analysis suggested that Rux may be involved in inhibiting Cdk1 activation until CycB–Cdk1 is exported from the nucleus to the cytoplasm. Two possible mechanisms of how Rux could suppress Cdk1-Cyclins in the nucleus could be considered. Rux may inhibit Cdk1–CycA activity in the nucleus. As the CycA is translated and activated earlier than CycB (White-Cooper et al., 1998, Foley, et al., 1999, Varadarajan, et al., 2016), Cdk1–CycB activity, a major driver of male meiosis, may be suppressed via inhibition of Cdk1–CycA by Rux until the complex is exported from the nucleus. Alternatively, Rux may directly suppress Cdk1–CycB in spermatocytes before meiosis. Rux can bind to CycB–Cdk1 and suppress its CycB-dependent kinase activity (Foley *et al*., 1999). However, the effects of Rux on mitotic cyclin–Cdk1 complexes opens up the possibility that it may also contribute to regulating entry into mitosis in *Drosophila* embryos (Sprenger *et al*., 1997). Whether *Rux* is involved in determining the timing of male meiosis should be investigated.

4.3. Rapid reentry of Cdk1–CycB into the nucleus may play an important role in the full-scale activation of Cdk1 with initial activity and meiotic initiation

Our observations indicate that nuclear reimport of CycB is a rapid process. The nuclear transfer machinery may be activated by Cdk1, thereby enabling its rapid nuclear-to-cytoplasmic transport. CycB1 is imported through direct interaction with importin β. Cdk1 phosphorylates importin β, stimulating interaction between importins α and β to accelerate protein transport (Moore *et al*., 1999, Takizawa *et al*., 1999, Guo *et al*., 2019). We noticed that importin β was involved in rapid nuclear import of CycB, although a typical NLS was not identified in *Drosophila* CycB. Importin β was not required for slow import in the G2 phase before centrosome separation, as the event was not affected in *Fs(2)*-silenced cells. Polo-like kinase suppresses nuclear export of cyclin B1–Cdk1 via phosphorylation of nuclear export signal of the cyclin in animal cells (Toyoshima-Morimoto et al., 2001, Lindqvist et al., 2009). This kinase is considered to facilitate rapid accumulation of CycB in the nucleus. However, *polo* may not play a critical role in rapid nuclear import of Cdk1–CycB at the onset of *Drosophila* male meiosis, because the silencing of *polo* did not affect meiotic initiation and its nuclear export did not change in *Nup62*-silenced cells.

We obtained evidence that subcellular localization of essential cell cycle regulators plays an important role in Cdk1 activation and meiotic initiation. Cdk1 needs to be activated in the cytoplasm during the G2/M transition; otherwise, meiosis cannot initiate properly. When Cdk1 remains in the nucleus, the level of Cdk1–CycB is reduced in the cytoplasm, becoming insufficient to initiate meiosis. If the positive regulators required for Cdk1 activation are localized in the cytoplasm, Cdk1 must be exported to the cytoplasm for activation. Conversely, if negative regulators are localized in the nucleus, they need to be released from Cdk1 for its activation. CAK and Twine were localized in the nucleus throughout the growth phase. Subcellular localization of these positive factors does not support the first possibility. By contrast, the negative regulators, Wee1/Myt1 was also predominantly localized in the nucleus. Rux is localized in the cytoplasm when CycA reenters the nucleus (Varadarajan et al., 2016). Before this developmental stage, the subcellular localization of Rux was not reported. However, we observed that *Rux* silencing rescued the accumulation of CycB–Cdk1 in the nucleus, thereby suggesting that the Cdk1 complex was suppressed by Rux until being released from the inhibitor.

Cell cycle regulation differs in some points between *Drosophila* male meiosis and mitosis. Before initiation of mitosis in animal cells, CycB migrates to the nucleus to avoid premature mitosis until DNA damage checkpoints are verified (Perry and Kornbluth, 2007). By contrast, initiation of meiosis may not be permitted until clearance of further conditions that the premeiotic spermatocytes should

Preprints (www.preprints.org) | NOT PEER-REVIEWED | Posted: 12 October 2023 doi:10.20944/preprints202310.0751.v1

fulfill, for example whether the cells are growing sufficiently. Several proteins and mRNAs required for meiotic divisions and post-meiotic events are synthesized during the growth phase (Inoue *et al*., 2012, White-Cooper *et al*., 2010). In a hypomorphic mutant for *eIF4G* encoding eukaryotic translation initiation factor, the growth of germline cells is inhibited. Neither meiosis nor sperm differentiation is observed in mutant testes (Franklin-Dumont *et al*., 2007, Baker *et al*., 2007). Therefore, Cdk1 activation that terminates the growth phase may need to be strictly regulated before meiosis, for example, at additional checkpoints that monitor cell growth.

4.4. Stepwise activation of Cdk1 is associated with nuclear-cytoplasmic shuttling of CycB mediated by the Nup62 subcomplex of the NPC, exportin, and importin β

We propose a new model regarding step-wise activation of Cdk1–cyclins, associated with nuclear-cytoplasmic shuttling of CycB (Figure 9). At a prolonged G2 phase in spermatocytes, Cdk1–CycB continues to be modified by Wee1/Myt1 and Twine in the cytoplasm. The complex has an intrinsic nature to temporally migrate to the nucleus. Simultaneously, it is exported more rapidly back to the cytoplasm through an exportin orthologue Emb via the Nup62 subcomplex in the NPC. Most of the kinase complexes are inactivated by Wee1/Myt1 that initially dominates over Twine, and further suppressed by Rux through suppression of Cdk1–cyclins (CycA or CycB) in the nucleus. Nevertheless, a small population of Cdk1–cyclins may execute some premeiotic events such as centrosome separation. With a sharp increase in CycB expression shortly before the onset of meiosis, a small population of active Cdk1 initiates the production of a large amount of active Cdk1 complex through activation of Twine and inactivation of the negative regulators. The kinase complex is rapidly imported into the nucleus via the Fs(2)Ket/importin β-mediated pathway. Through positive and double-negative feedback loops, resultant CycB–Cdk1 after completion of full-scale activation in the nucleus triggers meiotic initiation. Further investigation is warranted to validate this model.

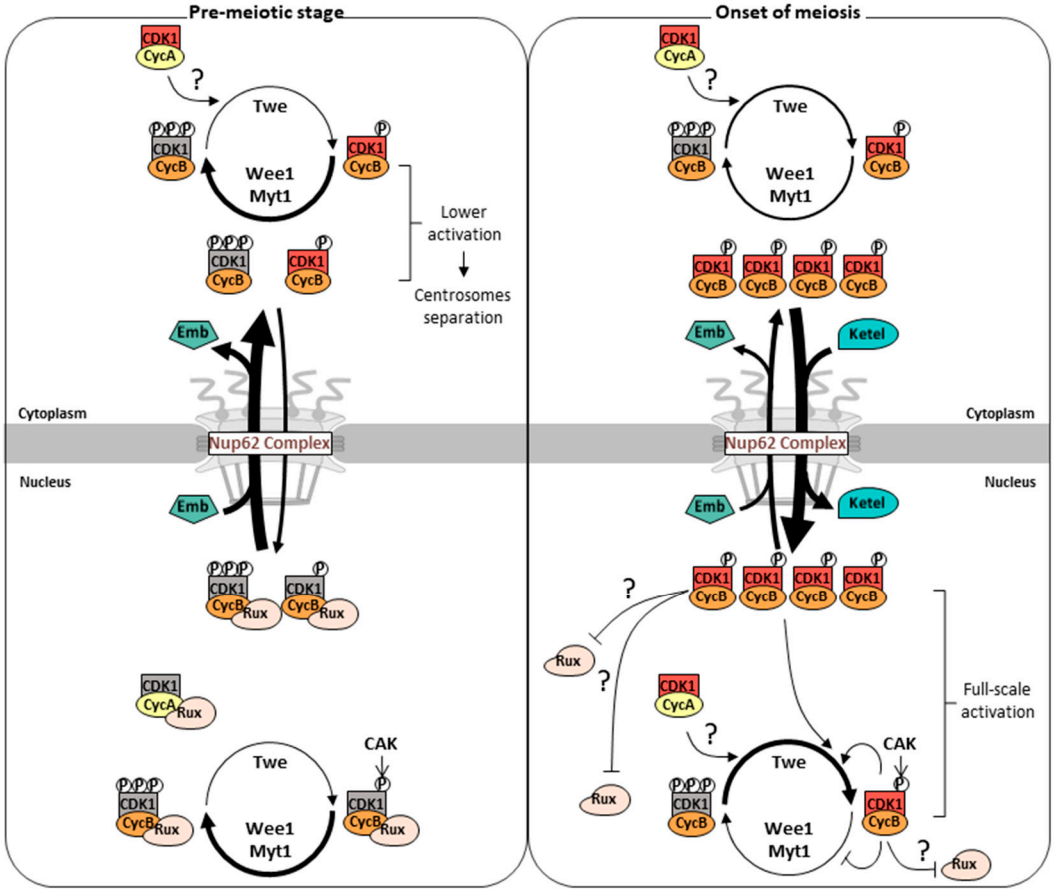

Figure 9. New model on the dynamics of CycB–Cdk1 shuttling in and out of the nucleus at interphase and its rapid nuclear reentry to initiate male meiosis in *Drosophila*. A model illustrating the dynamics

of CycB (orange) and Cdk1 (red) complex transport across the nuclear membrane (light gray) at premeiotic stage when nuclear export via the Nup62 subcomplex in the nuclear pore complex is continued (lefthand panel). Subsequently, the CycB–Cdk1 complex with complete modification essential for meiotic initiation is transported back into the nucleus to trigger meiotic division (right panel).

Supplementary Materials: The following supporting information can be downloaded at the website of this paper posted on Preprints.org. Figure S1: Effect of ectopic expression of normal CycB or NLS-CycB on their subcellular localization in mature spermatocytes.; Figure S2: The effect of *polo* silencing in spermatocytes on the G2/M progression in male meiosis.; Figure S3: Cellular localization of Polo-GFP in spermatocytes from S5 of the growth phase stages to the later ProI.; Figure S4: Detection of protein interaction between CycB and Polo-GFP by in situ proximity ligation assay.; Figure S5: Intracellular localization of Wee1 and Myt1, and detection of their close association with Cdk1 by *in situ* PLA in mature spermatocytes at S5, S6, and ProI.; Figure S6: Intracellular localization of Z600 protein in normal and *Nup62RNAi* mature spermatocytes, and immunostaining to detect colocalization of Z600 and CycB in the premeiotic cells.; Figure S7: Single spermatids cysts at onion stage in the testes harboring spermatocyte-specific depletion of components required for the nucleo-cytoplasmic transport.

Author Contributions: Conceptualization, Y.H.I. and K.Y.; methodology, K.Y.; validation, K.Y. and Y.H.I; formal analysis, and investigation, K.Y.; resources, Y.H.I.; data curation, Y.H.I.; writing—original draft preparation, K.Y. and Y.H.I.; writing—review and editing, Y.H.I.; supervision, Y.H.I.; project administration, Y.H.I.; funding acquisition, Y.H.I. All authors have read and agreed to the published version of the manuscript.

Funding: This study was partially supported by Grant-in-Aid for Scientific Research C (17K07500) to YHI. KY was supported by JST SPRING, Grant Number JPMJSP2107.

Institutional Review Board Statement: Not applicable.

Informed Consent Statement: Not applicable.

Data Availability Statement: The journal encourages all authors of articles published in MDPI journals to share their research data. In this section, please provide details regarding where data supporting reported results can be found, including links to publicly archived datasets analyzed or generated during the study. Where no new data were created, or where data is unavailable due to privacy or ethical restrictions, a statement is still required. Suggested Data Availability Statements are available in section "MDPI Research Data Policies" at https://www.mdpi.com/ethics.

Acknowledgments: We acknowledge Drs. J. Raff (University of Oxford), S. Campbell (Alberta University), E. Wieschaus (Princeton University), J. Großhans (The Philipps University of Marburg), V. Archambault (Montreal University), F. Sprenger (Universität Regensburg), and D. Glover (Cambridge University), Bloomington Drosophila Stock Center, Vienna Drosophila Resource Center, and Fly-ORF for providing fly stocks, plasmids, and antibodies.

Conflicts of Interest: The authors declare no conflict of interest.

References

1. Morgan, D.O. The Cell Cycle: Principles of Control (Primers in Biology), New Science Press Ltd. 2007. 297 pp. ISBN: 978-0-9539181-2-6.
2. Alberts, B.; Johnson, A.; Lewis, J.; Morgan. D.; Raff, M.; Roberts, K; Walter, P. (2017-08-07). Wilson J, Hunt T (eds.). Molecular Biology of the Cell (6th ed.). W.W. Norton & Company.
3. Liu, F.; Stanton, J.J.; Wu, Z.; Piwnica-Worms, H. The Human Myt1 Kinase Preferentially Phosphorylates Cdc2 on Threonine 14 and Localizes to the Endoplasmic Reticulum and Golgi Complex. Molecular and Cellular Biology 1997, 17, 571–583
4. Coulonval, K.; Kooken, H.; Roger, P.P. Coupling of T161 and T14 Phosphorylations Protects Cyclin B–CDK1 from Premature Activation. MBoC 2011, 22, 3971–3985
5. Ayeni, J.O.; Varadarajan, R.; Mukherjee, O.; Stuart, D.T.; Sprenger, F.; Srayko, M.; Campbell, S.D. Dual Phosphorylation of Cdk1 Coordinates Cell Proliferation with Key Developmental Processes in Drosophila. Genetics 2014, 196, 197–210
6. Kaldis, P. The Cdk-Activating Kinase (CAK): From Yeast to Mammals. CMLS, Cell. Mol. Life Sci. 1999, 55, 284–296
7. Dulić, V.; Stein, G.H.; Far, D.F.; Reed, S.I. Nuclear Accumulation of p21Cip1 at the Onset of Mitosis: A Role at the G2/M-Phase Transition. Molecular and Cellular Biology 1998, 18, 546–557

8. Dash, B.C.; El-Deiry, W.S. Phosphorylation of P21 in G2/M Promotes Cyclin B-Cdc2 Kinase Activity. Molecular and Cellular Biology 2005, 25, 3364–3387
9. Russo, A.A.; Jeffrey, P.D.; Pavletich, N.P. Structural Basis of Cyclin-Dependent Kinase Activation by Phosphorylation. Nat Struct Biol 1996, 3, 696–700
10. Lim, S.; Kaldis, P. Cdks, Cyclins and CKIs: Roles beyond Cell Cycle Regulation. Development 2013, 140, 3079–3093
11. Lindqvist, A.; Rodríguez-Bravo, V.; Medema, R.H. The Decision to Enter Mitosis: Feedback and Redundancy in the Mitotic Entry Network. Journal of Cell Biology 2009, 185, 193–202
12. Qian, J.; Winkler, C.; Bollen, M. 4D-Networking by Mitotic Phosphatases. Current Opinion in Cell Biology 2013, 25, 697–703
13. Hégarat, N.; Rata, S.; Hochegger, H. Bistability of Mitotic Entry and Exit Switches during Open Mitosis in Mammalian Cells. BioEssays 2016, 38, 627–643
14. Hiraoka, D.; Hosoda, E.; Chiba, K.; Kishimoto, T. SGK Phosphorylates Cdc25 and Myt1 to Trigger Cyclin B–Cdk1 Activation at the Meiotic G2/M Transition. Journal of Cell Biology 2019, 218, 3597–3611
15. Santos, S.D.M.; Wollman, R.; Meyer, T.; Ferrell, J.E. Spatial Positive Feedback at the Onset of Mitosis. Cell 2012, 149, 1500–1513
16. Maryu, G.; Yang, Q. Nuclear-Cytoplasmic Compartmentalization of Cyclin B1-Cdk1 Promotes Robust Timing of Mitotic Events. Cell Reports 2022, 41
17. Crncec, A.; Hochegger, H. Triggering Mitosis. FEBS Letters 2019, 593, 2868–2888
18. Pines, J.; Hunter, T. Cyclin-Dependent Kinases: A New Cell Cycle Motif? Trends in Cell Biology 1991, 1, 117–121
19. Hagting, A.; Karlsson, C.; Clute, P.; Jackman, M.; Pines, J. MPF Localization Is Controlled by Nuclear Export. The EMBO Journal 1998, 17, 4127–4138
20. Porter, L.A.; Donoghue, D.J. Cyclin B1 and CDK1: Nuclear Localization and Upstream Regulators. Prog Cell Cycle Res 2003, 5, 335–347
21. Gavet, O.; Pines, J. Progressive Activation of CyclinB1-Cdk1 Coordinates Entry to Mitosis. Developmental Cell 2010, 18, 533–543
22. Holt, J.E.; Weaver, J.; Jones, K.T. Spatial Regulation of APCCdh1-Induced Cyclin B1 Degradation Maintains G2 Arrest in Mouse Oocytes. Development 2010, 137, 1297–1304
23. Sigrist, S.; Ried, G.; Lehner, C.F. Dmcdc2 Kinase Is Required for Both Meiotic Divisions during Drosophila Spermatogenesis and Is Activated by the Twine/Cdc25 Phosphatase. Mechanisms of Development 1995, 53, 247–260
24. Courtot, C.; Fankhauser, C.; Simanis, V.; Lehner, C.F. The Drosophila Cdc25 Homolog Twine Is Required for Meiosis. Development 1992, 116, 405–416
25. Alphey, L.; Jimenez, J.; White-Cooper, H.; Dawson, I.; Nurse, P.; Glover, D.M. Twine, a Cdc25 Homolog That Functions in the Male and Female Germline of Drosophila. Cell 1992, 69, 977–988
26. White-Cooper, H.; Alphey, L.; Glover, D.M. The Cdc25 Homologue Twine Is Required for Only Some Aspects of the Entry into Meiosis in Drosophila. Journal of Cell Science 1993, 106, 1035–1044
27. White-Cooper, H.; Schäfer, M.A.; Alphey, L.S.; Fuller, M.T. Transcriptional and Post-Transcriptional Control Mechanisms Coordinate the Onset of Spermatid Differentiation with Meiosis I in Drosophila. Development 1998, 125, 125–134
28. Baker, C.C.; Gim, B.S.; Fuller, M.T. Cell Type-Specific Translational Repression of Cyclin B during Meiosis in Males. Development 2015, 142, 3394–3402
29. Inoue, Y.H.; Miyauchi, C.; Ogata, T.; Kitazawa, D. Dynamic alteration of cellular component of male meiosis in Drosophila. In Meiosis-Molecular Mechanisms and Cytogenetic Diversity; InTech: Rijeka, Croatia, 2012; pp. 953–979.
30. Cenci, G.; Bonaccorsi, S.; Pisano, C.; Verni, F.; Gatti, M. Chromatin and Microtubule Organization during Premeiotic, Meiotic and Early Postmeiotic Stages of Drosophila Melanogaster Spermatogenesis*. Journal of Cell Science 1994, 107, 3521–3534,
31. Azuma, M.; Ogata, T.; Yamazoe, K.; Tanaka, Y.; Inoue, Y.H. Heat Shock Cognate 70 Genes Contribute to Drosophila Spermatocyte Growth Progression Possibly through the Insulin Signaling Pathway. Development, Growth & Differentiation 2021, 63, 231–248
32. Hayashi, D.; Tanabe, K.; Katsube, H.; Inoue, Y.H. B-Type Nuclear Lamin and the Nuclear Pore Complex Nup107-160 Influences Maintenance of the Spindle Envelope Required for Cytokinesis in Drosophila Male Meiosis. Biology Open 2016, 5, 1011–1021
33. Okazaki, R.; Yamazoe, K.; Inoue, Y.H. Nuclear Export of Cyclin B Mediated by the Nup62 Complex Is Required for Meiotic Initiation in Drosophila Males. Cells 2020, 9, 270
34. Huang, J.; Raff, J.W. The Disappearance of Cyclin B at the End of Mitosis Is Regulated Spatially in Drosophila Cells. The EMBO Journal 1999, 18, 2184–2195

35. Schertel, C.; Huang, D.; Björklund, M.; Bischof, J.; Yin, D.; Li, R.; Wu, Y.; Zeng, R.; Wu, J.; Taipale, J.; Song, H.; Basler, K. (2013). Systematic screening of a Drosophila ORF library in vivo uncovers wnt/wg pathway components. Developmental Cell 2013, 25, 207–219.
36. Liu, B.; Gregor, I.; Müller, H.-A.; Großhans, J. Fluorescence Fluctuation Analysis Reveals PpV Dependent Cdc25 Protein Dynamics in Living Embryos. PLOS Genetics 2020, 16, e1008735
37. Oka, S.; Hirai, J.; Yasukawa, T.; Nakahara, Y.; Inoue, Y.H. A Correlation of Reactive Oxygen Species Accumulation by Depletion of Superoxide Dismutases with Age-Dependent Impairment in the Nervous System and Muscles of Drosophila Adults. Biogerontology 2015, 16, 485–501
38. Dienemann, A.; Sprenger, F. Requirements of Cyclin A for Mitosis Are Independent of Its Subcellular Localization. Current Biology 2004, 14, 1117–1123
39. Whitfield, W.G.; Gonzalez, C.; Maldonado-Codina, G.; Glover, D.M. The A- and B-Type Cyclins of Drosophila Are Accumulated and Destroyed in Temporally Distinct Events That Define Separable Phases of the G2-M Transition. The EMBO Journal 1990, 9, 2563–2572
40. Novak, Z.A.; Conduit, P.T.; Wainman, A.; Raff, J.W. Asterless Licenses Daughter Centrioles to Duplicate for the First Time in Drosophila Embryos. Current Biology 2014, 24, 1276–1282
41. Di Talia, S.; She, R.; Blythe, S.A.; Lu, X.; Zhang, Q.F.; Wieschaus, E.F. Posttranslational Control of Cdc25 Degradation Terminates Drosophila's Early Cell-Cycle Program. Current Biology 2013, 23, 127–132
42. Tanabe, K.; Awane, R.; Shoda, T.; Yamazoe, K.; Inoue, Y.H. Mutations in Mxc Tumor-Suppressor Gene Induce Chromosome Instability in Drosophila Male Meiosis. Cell Structure and Function 2019, 44, 121–135
43. Foley, E.; O'Farrell, P.H.; Sprenger, F. Rux Is a Cyclin-Dependent Kinase Inhibitor (CKI) Specific for Mitotic Cyclin–Cdk Complexes. Current Biology 1999, 9, 1392–1402
44. Gawliński, P.; Nikolay, R.; Goursot, C.; Lawo, S.; Chaurasia, B.; Herz, H.-M.; Kußler-Schneider, Y.; Ruppert, T.; Mayer, M.; Großhans, J. The Drosophila Mitotic Inhibitor Frühstart Specifically Binds to the Hydrophobic Patch of Cyclins. EMBO reports 2007, 8, 490–496
45. Gönczy, P.; Thomas, B.J.; DiNardo, S. Roughex Is a Dose-Dependent Regulator of the Second Meiotic Division during Drosophila Spermatogenesis. Cell 1994, 77, 1015–1025
46. Hagting, A.; Jackman, M.; Simpson, K.; Pines, J. Translocation of Cyclin B1 to the Nucleus at Prophase Requires a Phosphorylation-Dependent Nuclear Import Signal. Current Biology 1999, 9, 680–689
47. Varadarajan, R.; Ayeni, J.; Jin, Z.; Homola, E.; Campbell, S.D. Myt1 Inhibition of Cyclin A/Cdk1 Is Essential for Fusome Integrity and Premeiotic Centriole Engagement in Drosophila Spermatocytes. MBoC 2016, 27, 2051–2063
48. Sprenger, F.; Yakubovich, N.; O'Farrell, P.H. S-Phase Function of Drosophila Cyclin A and Its Downregulation in G1 Phase. Current Biology 1997, 7, 488–499
49. Moore, J.D.; Yang, J.; Truant, R.; Kornbluth, S. Nuclear Import of Cdk/Cyclin Complexes: Identification of Distinct Mechanisms for Import of Cdk2/Cyclin E and Cdc2/Cyclin B1. Journal of Cell Biology 1999, 144, 213–224
50. Takizawa, C.G.; Weis, K.; Morgan, D.O. Ran-Independent Nuclear Import of Cyclin B1–Cdc2 by Importin β. Proceedings of the National Academy of Sciences 1999, 96, 7938–7943
51. Guo, L.; Mohd, K.S.; Ren, H.; Xin, G.; Jiang, Q.; Clarke, P.R.; Zhang, C. Phosphorylation of Importin-α1 by CDK1–Cyclin B1 Controls Mitotic Spindle Assembly. Journal of Cell Science 2019, 132, jcs232314
52. Toyoshima-Morimoto, F.; Taniguchi, E.; Shinya, N.; Iwamatsu, A.; Nishida, E. Polo-like Kinase 1 Phosphorylates Cyclin B1 and Targets It to the Nucleus during Prophase. Nature 2001, 410, 215–220
53. Perry, J.A.; Kornbluth, S. Cdc25 and Wee1: Analogous Opposites? Cell Division 2007, 2, 12
54. White-Cooper, H. Molecular Mechanisms of Gene Regulation during Drosophila Spermatogenesis. Reproduction 2010, 139, 11–21
55. Franklin-Dumont, T.M.; Chatterjee, C.; Wasserman, S.A.; DiNardo, S. A Novel eIF4G Homolog, Off-Schedule, Couples Translational Control to Meiosis and Differentiation in Drosophila Spermatocytes. Development 2007, 134, 2851–2861
56. Baker, C.C.; Fuller, M.T. Translational Control of Meiotic Cell Cycle Progression and Spermatid Differentiation in Male Germ Cells by a Novel eIF4G Homolog. Development 2007, 134, 2863–2869
57. Huang, J.; Gujar, M.R.; Deng, Q.; Y Chia, S.; Li, S.; Tan, P.; Sung, W.-K.; Wang, H. Histone Lysine Methyltransferase Pr-Set7/SETD8 Promotes Neural Stem Cell Reactivation. EMBO reports 2021, 22, e50994
58. Ni, J.-Q.; Zhou, R.; Czech, B.; Liu, L.-P.; Holderbaum, L.; Yang-Zhou, D.; Shim, H.-S.; Tao, R.; Handler, D.; Karpowicz, P.; et al. A Genome-Scale shRNA Resource for Transgenic RNAi in Drosophila. Nat Methods 2011, 8, 405–407
59. Khalil, B.; Chhangani, D.; Wren, M.C.; Smith, C.L.; Lee, J.H.; Li, X.; Puttinger, C.; Tsai, C.-W.; Fortin, G.; Morderer, D.; et al. Nuclear Import Receptors Are Recruited by FG-Nucleoporins to Rescue Hallmarks of TDP-43 Proteinopathy. Molecular Neurodegeneration 2022, 17, 80

disclaim responsibility for any injury to people or property resulting from any ideas, methods, instructions or products referred to in the content.